iScience, Volume *23*

Supplemental Information

A 3D Bioprinter Specifically Designed for the High-Throughput Production of Matrix-Embedded Multicellular Spheroids

Robert H. Utama, Lakmali Atapattu, Aidan P. O'Mahony, Christopher M. Fife, Jongho Baek, Théophile Allard, Kieran J. O'Mahony, Julio C.C. Ribeiro, Katharina Gaus, Maria Kavallaris, and J. Justin Gooding

Supplemental Data Items

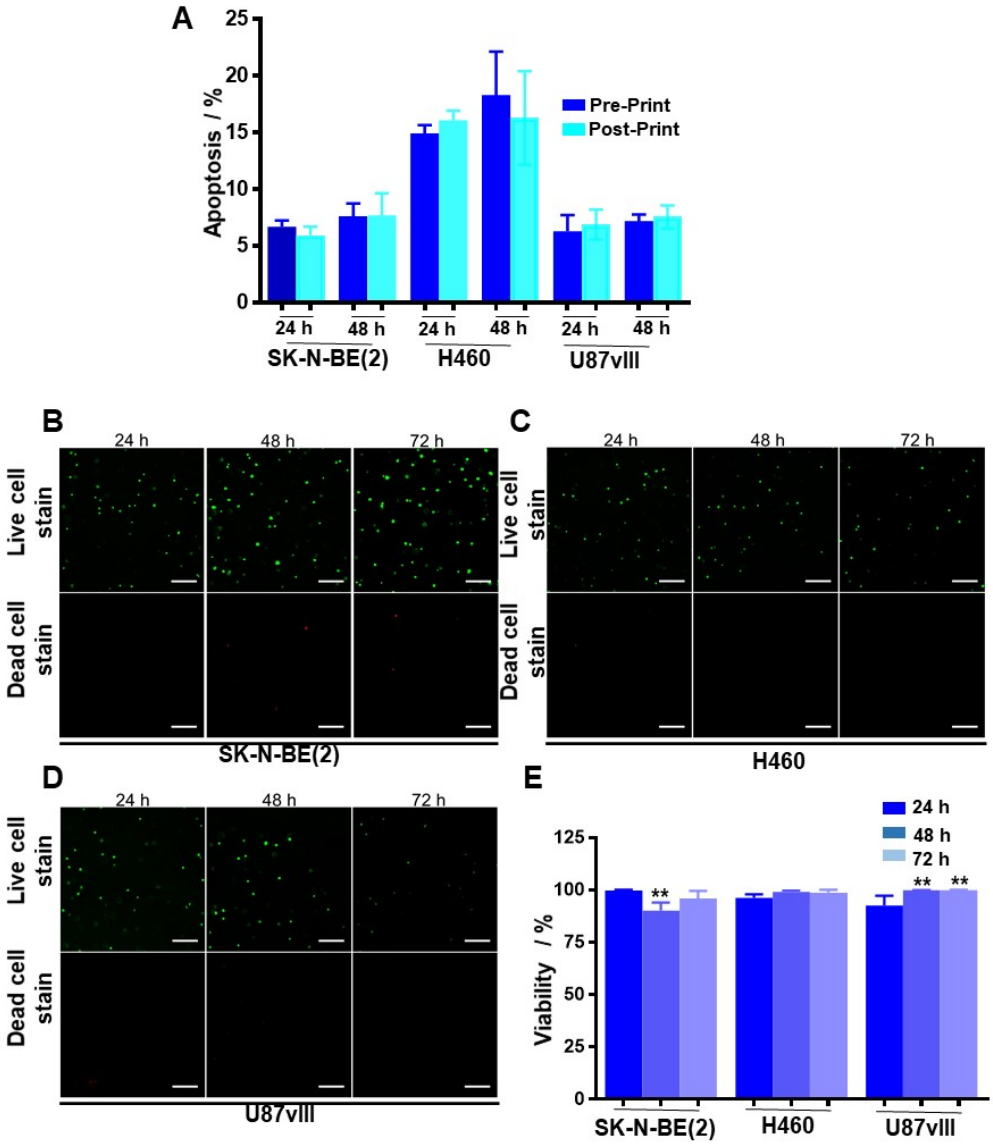

Figure S1. Cell viability and apoptosis studies on neuroblastoma (SK-N-BE(2)), non-small cell lung cancer (H460) and glioblastoma (U87vIII) cells (**A**) Annexin V apoptosis assay showing no visible effect of bioprinting on the cells when compared to the non-printed cells. 3D bioprinted neuroblastoma (SK-N-BE(2)), non-small cell lung cancer (H460) and glioblastoma (U87vIII) 3D cell encapsulation assay. Cells were dispersed in the bioink at 2 x 10^8 cells/mL and bioprinted, together with the activator, to embed single cells inside the 3D hydrogel matrix. (*n* = 3, One-way ANOVA; n.s.) (**B-D**) Live/dead assay staining on the samples after 24, 48, and 72 h incubation, using calcein AM (green) that stained living cells and ethidium homodimer (red), which stains dead cells. Scale bar = 250 µm. (**E**) Counted number of cells from the microscopy images showing that viability of > 95% was observed in all samples and across three different cell lines. (*n* = 3, One-way ANOVA; SK-N-BE(2): **P < 0.05, H460: n.s., U87vIII: **P < 0.05). Results are means ± SEM. Related to Figure 1.

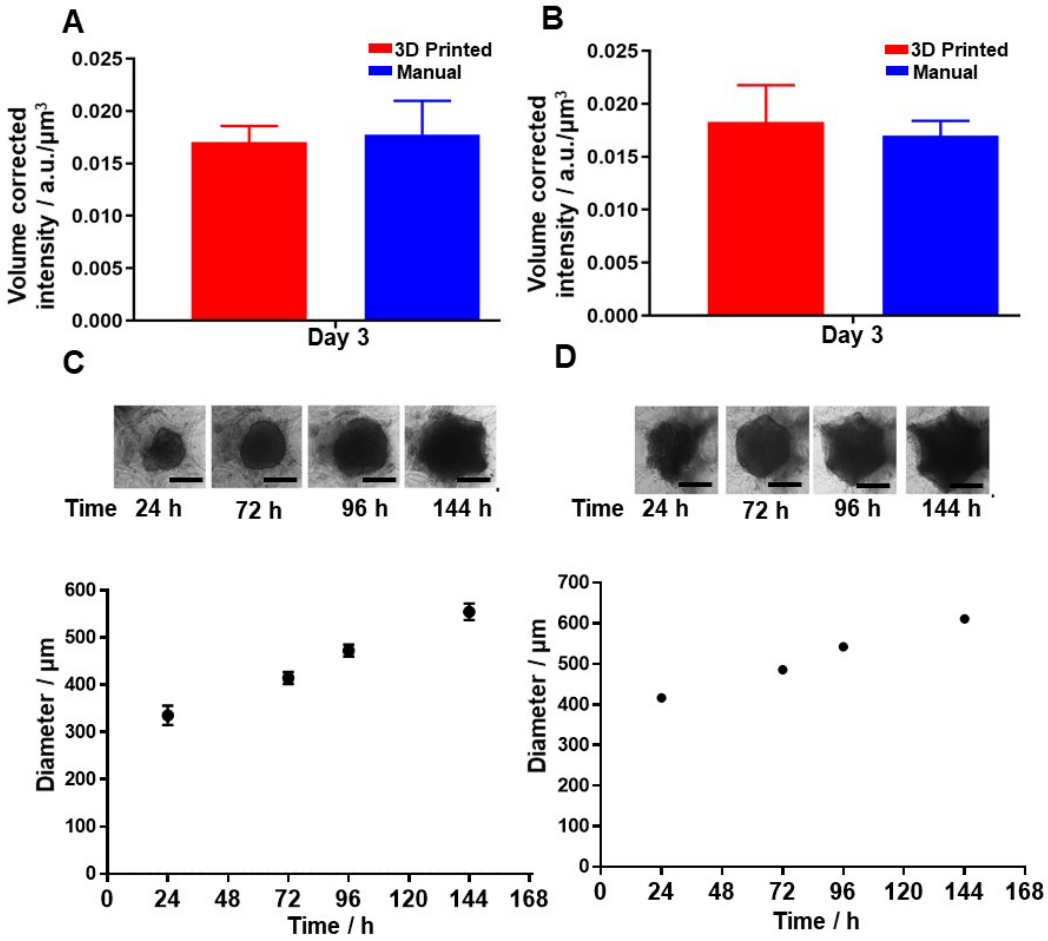

Figure S2. **Spheroid viability and growth studies on non-small cell lung cancer (H460) and glioblastoma (U87vIII) cells** (**A**) 3D bioprinted H460 showed significantly higher viability over manually prepared spheroids at day 3 (*n* = 3, one-way ANOVA; n.s.) (**B**) U87vIII spheroids and manually formed spheroids had similar viability at day 3 (*n* = 3, one-way ANOVA; n.s.)(**C**) The formation and growth of H460 and (**D**) U87vIII spheroids over a period of 144 h from an estimated 23,750 cells printed for H460 and approximately 45,000 cells for U87vIII. In all cases, spheroids formed after 24 h and conformed to the shape of the hydrogel matrix cup after 144 h. (*n* = 6 experimental replicates, scale bars = 200 µm). Results are means ± SEM. Related to Figure 1.

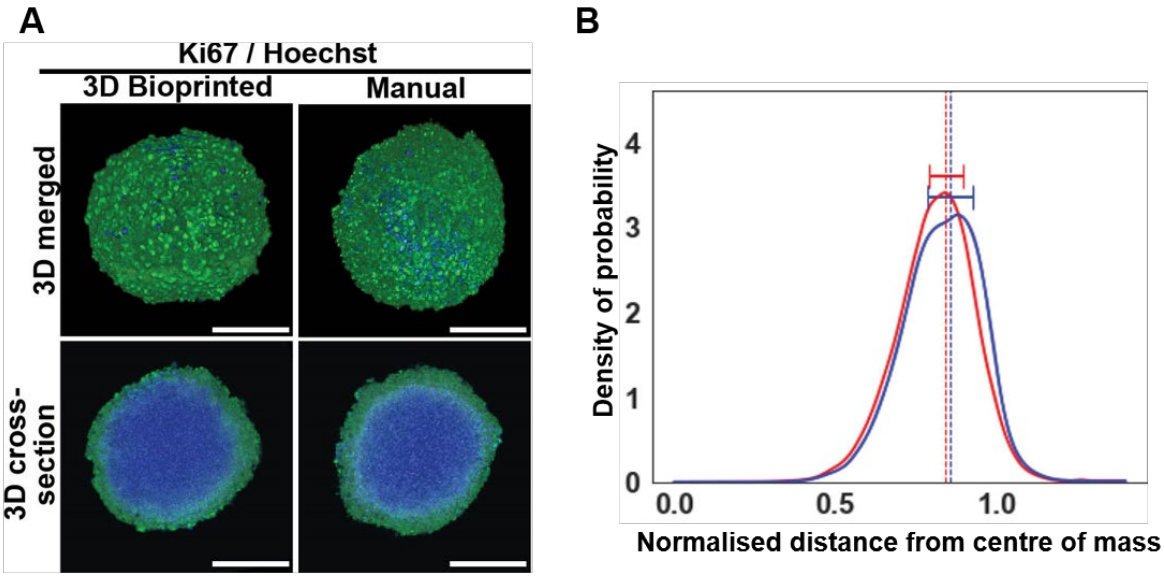

Figure S3. Ki-67 immunofluorescence analysis of the 3D bioprinted spheroids after 6 days of incubation. (**A**) Cells within the spheroids were labelled with α-Ki67 antibody (green), indicating cell proliferation and the DNA dye Hoechst 33342 (blue). The 3D cross-section images showed that the location of proliferating cells was consistent with the observed results on day 3 spheroids. (*n* = 2, scale bars = 300 μm) (**B**) Averaged, normalized distance distribution of the proliferating cells in both 3D bioprinted (red) and manual (blue) spheroid, with an x-axis value of 0 indicating the centre of the spheroid and 1 indicating the periphery of the spheroid. The dashed lines indicate the distance with maximum probability, with the standard deviation presented for both spheroid sets. Results are means ± SEM. Related to Figure 2.

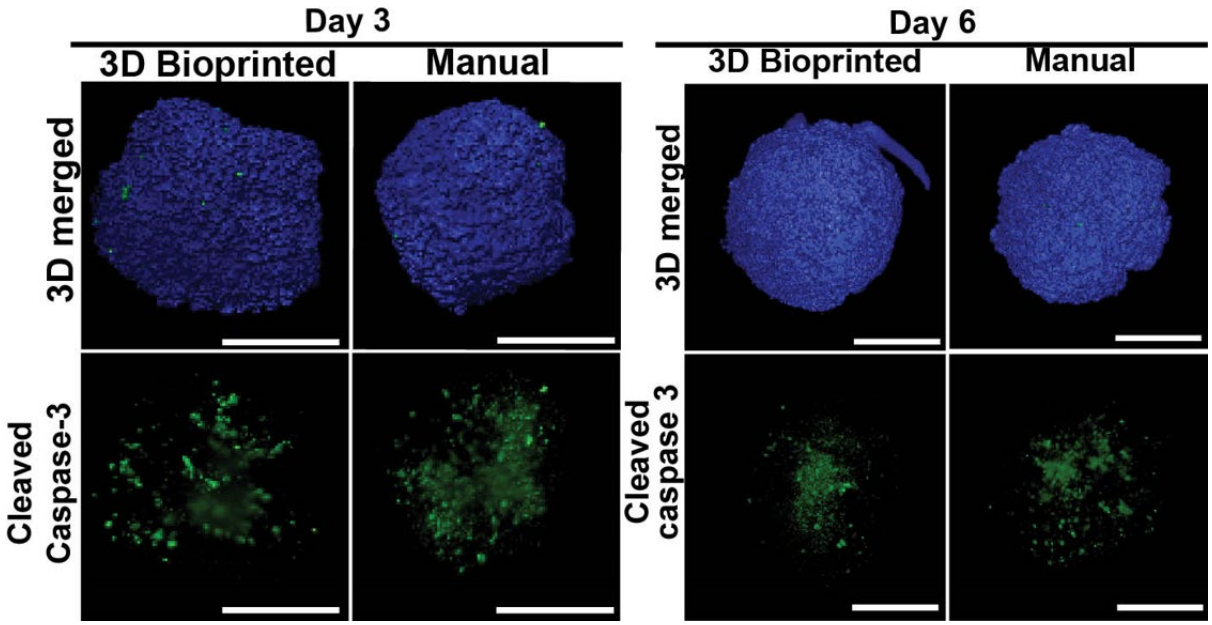

Figure S4. 3D rendered images of the 3D bioprinted and manual SK-N-BE(2) spheroids, labelled with α-cleaved caspase-3 antibody (green) and Hoechst 33342 (blue) and the corresponding 3D cleaved caspase-3 channel, after 3 and 6 days of incubation. The cleaved caspsase-3 channel images showing the location of apoptotic cells within the spheroids. Scale bars = 300 μm. Related to Figure 2.

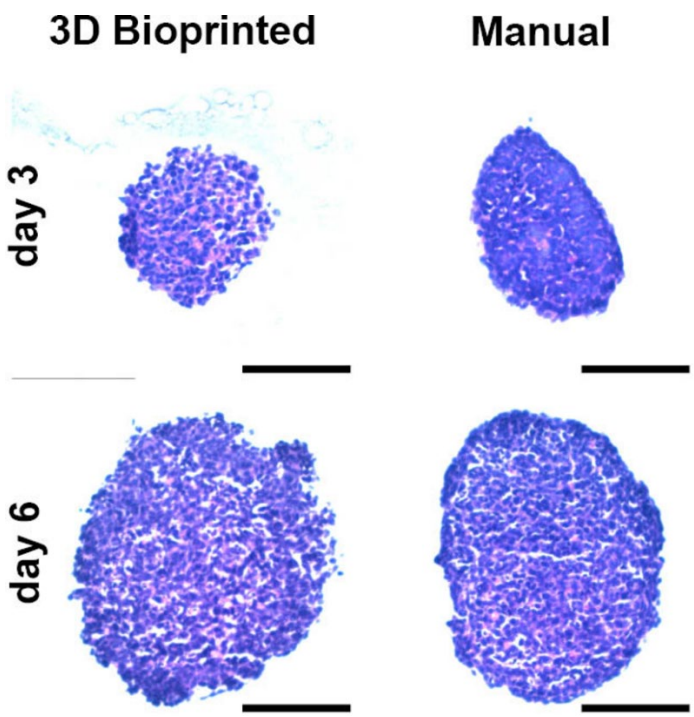

Figure S5. Micrographs of the H&E slices of the 3D bioprinted and manual SK-N-BE(2) spheroids at day 3 and day 6. Scale bars = 300 μm. Related to Figure 2.

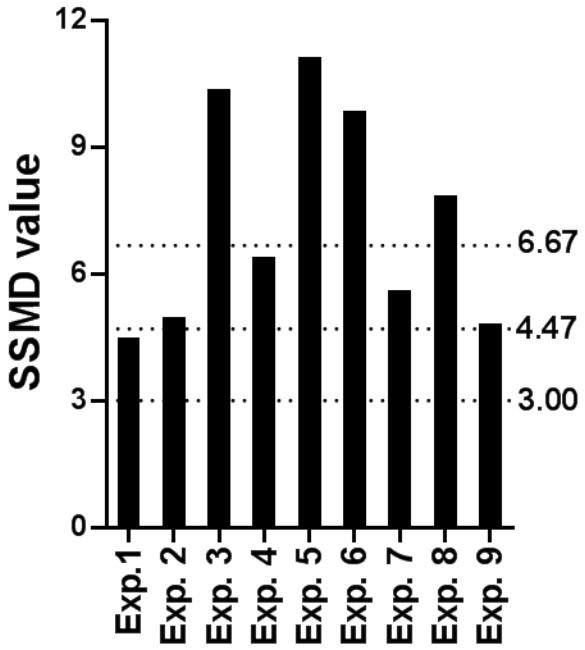

SSMD	QC Interpretation
SSMD ≥ 6.67	Excellent (E)
6.67 > SSMD ≥ 4.7	Good
4.7 > SSMD ≥ 3	Acceptable (A)
SSMD < 3	Poor (P)

Figure S6. Calculated SSMD values for each assay conducted for all HTS experiments, with the dotted line outlining the threshold value for the quality control (QC) interpretation. The corresponding table summarises the theoretical values of the quality control QC tests. For the SSMD value calculation, (*n* = *min. 6*). Related to Figure 3.

Transparent Methods

Materials

Dulbecco's Phosphate Buffer Saline (no calcium, no magnesium, DPBS, ThermoFisher Scientific), Dulbecco's Modified Eagle Medium (DMEM, ThermoFisher Scientific), Roswell Park Memorial Institute 1640 (RPMI, ThermoFisher Scientific), Fetal Calf Serum (FCS, Bovogen), Penicillin-Streptomycin (Pen-Strep, 10,000 U/mL, ThermoFisher Scientific), trypsin-EDTA (ThermoFisher Scientific) , ethanol (Univar), Triton-X (Sigma Aldrich), Bovine Serum Albumin (BSA, Sigma Aldrich) were used as received.

Bespoke 3D bioprinter

3D cell culture models were bioprinted using a non-contact drop-on-demand 3D bioprinter (now manufactured by Inventia Life Science). The bioprinter incorporates a flyby or scanning printhead that prints directly onto the substrate while in motion, allowing the printing of 12 wells (across a row of a 96-well plate) to be printed in the same amount of time as a single well. It comprises of a 2-axis motion control system, a droplet dispensing system and a pressure regulation system to control pressure in the fluid reservoirs. The bioprinter facilitates printing onto many types of multi-well plates. The 2-axis linear motion positioning system is capable of accurately positioning droplets on the substrate at a resolution of 20 µm along each axis. The droplet dispensing system consists of multiple independently addressable microvalves. Inks are primed into the nozzles from a bioprinting cartridge. The desired droplet volume can also be adjusted using the backpressure in the fluid reservoir and the microvalve opening time.

Preparation of the bioink, activator and chelating solutions

Three different ink solutions were used to produce the 3D spheroid assay. The bioink was prepared by mixing sodium alginate (FMC BioPolymer) in a 70/30 v/v% mixture of Milli-Q water and DPBS at 2 wt% for 16 h. The activator was prepared by mixing calcium chloride (Anhydrous, Sigma Aldrich) in Milli-Q water at 4 wt%. To make the chelating solution, sodium citrate (Sigma Aldrich) was dissolved in DPBS at 200 mM. All solutions were sterilised by filtration through a 0.22 µm syringe filter prior to use. The bioink was stored at 4 ^{o}C, while other solutions were stored at room temperature.

Cell culture

SK-N-BE(2) (human neuroblastoma) and U87vIII (human glioblastoma) cells were maintained in 10% fetal calf serum (FCS)/ DMEM at 37 °C/5% CO_2. Human non-small cell lung cancer H460 cells were cultured in 10% fetal calf serum (FCS)/RPMI at 37 °C/5% CO_2. Cell lines are routinely screened and free of mycoplasma contamination.

Cell viability and cell death assays

Trypan blue exclusion study was used to assess the viability of cells pre and post printing. SK-N-BE(2), H460 or U87vIII cells were harvested from 6-well plates using trypsin-EDTA and pelleted using centrifugation at 423 g. Cells were resuspended in bioink to a concentration of 2 x 10^8 cells/mL. The printed samples were cells passed through the 3D bioprinter while non-printed referred to manually pipetted cells. Dead cells were identified using 0.4% trypan blue stain (Invitrogen). Cell counts were obtained by counting the number of live and dead cells in each sample. Percentage cell viability was determined by dividing the total number of live cells by the total number of cells (live + dead).

To investigate the potential impact of the printing on apoptotic cell death, SK-N-BE(2), H460 or U87vIII cells were resuspended in a bioink to a concentration of 2 x 10^8 cells/mL. As controls, SK-N-BE(2), H460 or U87vIII cells were seeded into 6-well plates at 2 x 10^6 cells/well and incubated at 37°C/5% CO_2 for 24 h and 48 h. Cells pre- and post-printing were harvested as described above and stained with PE Annexin V (BD Biosciences), 7-aminoactinomycin D (7-AAD) (BD Biosciences), both PE Annexin V and 7-ADD or neither for 15 min at 37 °C in the dark. Apoptosis levels were measured by flow cytometry and analysed using FlowJo.

3D bioprinting of cancer spheroids

Bioink and activator were brought up to room temperature prior to printing. 3D bioprinter surfaces were sterilised by 70% ethanol wiping. The cartridges, fluidics and microvalves were sterilised by 70% ethanol (10 mL) and sterile Milli-Q water (10 mL) flushing. The bioink (1 mL) and activator (1 mL) were then pipetted into their respective cartridges.

Bioprinting structure definition and printing execution were conducted using the proprietary custom-made software by Inventia Life Science. The bioprinting pressure set to 1.45 kPa and 0.55 kPa for the

bioink and activator nozzle, respectively. Prior to initiating the printing process, spittooning was done on each microvalve to bring the inks into the nozzle and to ensure consistent ejection of liquid droplets. The hydrogel matrix printing process was as follow: a drop of activator (18.5 nL) was initially printed at the desired location which was quickly followed by printing a drop of the complementing bioink (65.3 nL) at the same location to initiate the crosslinking process. This process was repeated until the desired alginate hydrogel matrix structure was completed. Variation on the size of the 3D bioprinted cups was achieved by altering the microvalves opening time, in which larger opening time was used to achieve a smaller cup and vice versa.

Once the hydrogel mould printing has been completed, 50 µL of cell-laden ink of either SK-N-BE(2), H460 or U87vIII at 250 million cells/mL was pipetted into the printing cartridge, primed into the nozzle, pressurised to 0.59 kPa and spittooned. Five cell-laden ink droplets (19 nL each) were then bioprinted dropwise at 1 Hz into the hydrogel matrix cup. Finally, the bioprinting process was completed by the printing of the top layer of the alginate hydrogel matrix structure. At the completion of the printing process, 200 µL 10%FCS/DMEM (supplemented with Pen-Strep) was added manually in each individual well using a multi-channel pipette. The plate was then ready for incubation at 37 °C/5% CO_2 for desired time depending on the experiment.

Manual cancer spheroid formation
Manual spheroids were prepared using ultra-low attachment (ULA) 96-well round-bottomed plates (Corning) using the previously described method (Fife et al., 2017). Briefly, the optimised cell number for each cell line (SK-N-BE(2), H460 or U87vIII) were pipetted into the ULA plate and cultured in their respective media (200 µL) for 3 or 6 days at 37 °C/5% CO_2.

3D bioprinted spheroid recovery from the hydrogel matrix
Sterile chelating solution was used to recover the 3D bioprinted spheroids from the hydrogel matrix. The incubating media of the 3D bioprinted spheroids in the hydrogel matrix, after the desired incubation time, was firstly removed using a multi-channel pipette. 100 µL of the chelating solution was added into each well and the sample was incubated for 2 min at room temperature to dissociate the hydrogel matrix. After two minutes, the content of the well was carefully transferred into a microcentrifuge tube (Eppendorf) for further analysis.

H&E staining
Both the 3D bioprinted and the manually prepared SK-N-BE(2) neuroblastoma spheroids were fixed in 4% paraformaldehyde (PFA, Electron Microscopy Sciences) diluted in 1% Triton (Sigma-Aldrich) in DPBS for 2 days at 4 °C. The fixed spheroids were first embedded in a small amount of alginate hydrogel to hold them in place in a Tissue-Tek cryomolds (VWR), which were subsequently filled with 500 µL of 4 w/v% agarose (AppliChem). Solidified blocks were transferred to 50% ethanol for 1 h and stored in 80% ethanol. Paraffin embedding, sectioning and H&E staining of spheroids were performed as previously described (28).

CellTiter-Glo® 3D Viability assay
Two different variations of the CellTiter-Glo® 3D Viability assay (Promega) were used in this study. Assessment of the viability of manual spheroids and 3D bioprinted spheroids recovered from the hydrogel matrix as per the manufacturer's protocol in a 96-well solid white flat bottom plate (Corning). Briefly, spheroids were treated with 100 µL CellTiter-Glo® 3D solution in 96-well plates. Plates were incubated for 1 hour at room temperature on a Ratek microtiter PCR plate shaker at 30 rpm, prior to reading plates. Luminescence readings were obtained using the Perkin Elmer Victor3 plate reader. A standard built in protocol using appropriate filters were used to measure luminescence values. Average value of 3 luminescence readings were used as the final value. Spheroids treated with 0.4 mM doxorubicin (Teva Pharmaceuticals) for 1 h at room temperature were used as a positive control for cell death.

To consider the spheroid size variation between the 3D bioprinted and manual spheroids, the luminescence values were normalised to the volume of the spheroids. The volumes of the spheroids were calculated using the diameter of the spheroids obtained using a bright-field microscope and under the assumption that every spheroid was spherical. The spheroid volume-normalised luminescence values were further normalised to the manually generated spheroid.

In order to develop an HTS readout assay for our CellTiter-Glo® 3D protocol described above, we made slight modifications to the protocol. 25 µL of CellTiter-Glo® 3D solution was diluted in 175 µL of DPBS

to obtain a total of 200 µL of final solution for each well of a 96-well plate. 3D bioprinted spheroids in 96-well optical-bottom black plates (Cell Carrier, Perkin Elmer) were tested in situ using the CellTiter-Glo® 3D assay. Luminescence readings were performed following the same protocol as described above.

Drug penetration assay

To determine the ability of a fluorescent chemotherapy drug doxorubicin to penetrate spheroids, 3D bioprinted spheroids recovered from the hydrogel matrix and the manually prepared spheroids were placed in an ultra-low attachment 96-well round bottom well plate (Corning). Spheroids were then incubated with 3.68 µM doxorubicin in 10%FCS/DMEM for 2 h at 37 °C. The spheroids were then imaged every 2 h for 10 h using ZEISS LSM 880 with Airyscan confocal microscope. Images were taken using 10x objective, Argon laser (488nm) and transmitted light (bright field). Z stacks were defined from the bottom to the middle of the spheroids. For every time point, an image stack on the z-axis was taken. The microscope incubator was set to 37 °C/5% CO_2.

Fluorescence activated cell sorting (FACS) analysis for quantitative cell analysis

We investigated the expression of different cellular biomarkers using FACS analysis. Spheroids were treated with trypsin-EDTA for 20 mins at room temperature to separate into single cells, followed by neutralisation of trypsin-EDTA using 10% FCS/DMEM. Cells were spun down at 423 g and washed once with DPBS. Cell fixing was done by firstly suspending cell pellets in 4% PFA for 20 mins at room temperature. Cells were then pelleted at 423 g and washed twice with DPBS. Fixed cells were permeabilised with 0.1% Triton/DPBS for 10 mins at room temperature, washed twice with DPBS and blocked with 2%BSA in DPBS for 1 h at room temperature. α-cleaved caspase-3 (Cell Signalling Technology), α-HIF1α (abcam) or α-CD133 antibodies (abcam) diluted to 1/100 with 2% BSA/DPBS solution were incubated overnight with the cells. After removing excess primary antibody, the samples were stained with Alexa Fluor 488 labelled Goat anti-Rabbit IgG secondary antibody (ThermoFisher Scientific).

Positive staining was determined by flow cytometer BD FACSCanto using the 488 laser and analysed using FlowJo. Single cells were defined using Area Scaling Strategy (FCS-A vs FCS-H). Total Events (area based) were presented on the x-axis (FCS-A) and the events detected in the 488 nm laser channel were presented on the y-axis. Unstained cells used as negative control were used to set the baseline for the y-axis detected events and the percentages of positive cells above the baseline were shown in bar graphs as a direct comparison between manual and 3D printed cells.

Immunofluorescence staining

Fixation and immunofluorescence protocols for light-sheet microscopy were adapted from a previously described protocol (Weiswald et al., 2010). To improve penetration of staining reagents to the core of the spheroids, simultaneous fixation and permeabilising was performed on 3D spheroids in 4% PFA/1% Triton-X/DPBS solution for 3 days at 4 °C. Spheroids were washed once with DPBS after removing the fixation media and stored in 0.1% Triton-X/DPBS at 4 °C. Fixed and permeabilised spheroids were blocked in 2% BSA in 0.1% Triton/DPBS for 3 days at 4 °C. To remove excess blocking solution, the samples were washed once with 0.1% Triton/DPBS.

To stain spheroids with α-Ki67/Hoechst 33342 or α-cleaved caspase3/Hoechst 33342, blocked spheroids were firstly incubated for 2 days at 4 °C with α-Ki67 (Abcam, stock concentration 0.031 mg/mL) or α-cleaved caspase3 (Cell Signalling Technology, stock concentration is not provided by the manufacturer) antibodies. The primary antibodies working solution was prepared by diluting the stock solution in 0.1% Triton/DPBS at 1/100. After incubation, excess primary antibodies were removed by washing the samples twice with 0.1% Triton/DPBS. Subsequently, the samples were incubated with 2 µg/mL Alexa Fluor 488 labelled Goat anti-Rabbit IgG secondary antibody (ThermoFisher Scientific, stock solution, 2mg/mL) prepared by mixing the stock solution in 0.1% Triton/DPBS at 1/100 and 0.2 mM Hoechst 33342 (ThermoFisher Scientific, stock concentration 20 mM) prepared by mixing the stock solution in 0.1% Triton/DPBS at 1/100, at 4 °C, overnight. Finally, the stained spheroids were washed twice with 0.1% Triton/DPBS.

To prepare phalloidin/Hoechst 33342 stained spheroids, blocked spheroids were firstly stained with phalloidin conjugated to Alexa Fluor® 568 (ThermoFisher Scientific) under vigorous shaking at 4 °C, overnight. Phalloidin working solution (0.31 µM) was prepared by mixing 5 µL of phalloidin conjugated to Alexa Fluor® 568 stock solution (stock concentration; 6.6 µM) in 100 µL of 0.1% Triton/DPBS. After incubation, the spheroids were washed twice with 0.1% Triton/DPBS to remove excess phalloidin.

Nuclei were labelled by incubating phalloidin-labelled spheroids in Hoechst 33342 (0.2 mM) overnight at 4 ^{o}C on a shaker.

For Lattice light sheet imaging, the above method to prepare phalloidin-stained spheroids was followed to produce spheroids stained with phalloidin and. To stain the nuclei, phalloidin-stained spheroids were incubated in 0.167 µM SYTOX green (ThermoFisher Scientific) overnight at room temperature and protected from light. SYTOX green working solution was prepared by diluting SYTOX green (5 mM stock concentration) in DPBS at 1:30,000. After staining with SYTOX green, the spheroids were washed twice with DPBS and used immediately for lattice light sheet imaging.

Light-sheet microscopy

The samples stained with appropriate markers were resuspended in 1% low melt agarose (AppliChem) and placed in ZEISS blue capillaries (size 4). ZEISS Lightsheet Z.1. (Carl Zeiss Microscopy GmbH, Jena, Germany) with 20x/1.0 (water, nd = 1.33) detection objective and two-sided 10x/0.2 illumination objectives equipped with two PCO EDGE 4.2 cameras was utilised to image two angles (0^0 and 180^0) of the spheroids from two sides (right and left). Laser lines 405 nm/50 mW, 488 nm/50 mW and 561 nm/50 mW were used with beam splitters/emission filters SBS LP 490/ BP 420-470, SBS LP 490/BP 505-545 and SBS LP 560/ LP 585 respectively. To fuse the right and the left sides of the images either manual dual side fusion or online dual side fusion was performed using Zen(black) (Carl Zeiss Microscopy GmbH) software package according to manufacturer's instructions. To fuse the image stacks obtained from the two angles, software provided by the BioMedical Imaging Facility of University of New South Wales, Sydney, Australia was utilised.

Lattice light-sheet microscopy

In order to investigate the compactness of cells within the spheroids we used lattice light sheet microscopy. Recovered 3D bioprinted spheroids, stained with phalloidin/SYTOX green prepared as described previously were carefully placed on top of a 0.01% poly-L-lysine (Sigma Aldrich) coated 5 mm round coverslip. Prepared samples were subsequently imaged using a lattice light-sheet microscope (Intelligent Imaging Innovations Inc.). The microscope generated 1 µm thick light-sheets with a square lattice configuration in dithering mode. Images were acquired with two ORCA-Flash 4.0 scientific complementary metal-oxide semiconductor (sCMOS) cameras (Hamamatsu). Each camera acquired a single colour channel sequentially to build up a respective 3-dimensional image. Imaging planes were exposed for 20 ms with 488 nm or 642 nm laser light. Spheroids were imaged on a piezo sample stage with 150 nm-step movement, thereby capturing a volume of ~ 50 × 50 × 50 µm (512 × 512 × 333 pixels) within 20-25 s. The top edge of the spheroid was selected for assessing the imaging depth (~ 50 µm). Acquired images were saved as TIFF files, with each plane of a volume corresponding to a cross-section of the imaged sample. The acquired images in the raw data appeared as a shear-transformed projection of the sample because the samples visualised in scan mode were scanned at a slanted angle to the coverslip of 31.5°. To compensate this coordinate distortion, images were de-skewed using inverse shear transform (Slidebook6, 3i). De-skewed volumes were then deconvolved with Slidebook using the constrained iterative deconvolution algorithm and an experimental point spread function generated with 200 nm fluorescent beads (ThermoFisher Scientific).

Image analysis using Python

A python script employing the OpenCV Python binding library (Bradski, 2008) and the python-bioformats library was used to analyse the image sets of the Hoechst fluorescent channel to obtain the coordinates of each fluorescent cells in a 3-dimensional space. For each *z*-layer planar image, the script equalised the images' histogram, applied a Gaussian adaptive threshold using the "adaptiveThreshold" function and conducted a morphological closing transformation using the "morphologyEx" function to obtain a binary image of white blobs that represented the fluorescent cells. Into the binary image, a mask was applied and the "SimpleBlobDetector" function was used to find the bright cells surrounded by a black background. The coordinates at the centre of the blobs were recorded as the positions of the fluorescent cells' centre of mass in the 2D *x*-*y* plane. As the process was repeated through all *z*-slices, repeated coordinates were removed. For the instance where repeated coordinates that represent one cell distributed in multiple *z*-slices, only the middle occurrence was kept to obtain the position of the cell centres of mass in 3D. The output of the analysis consisted of the recorded positions and sizes in µm, based on the OME-XML metadata conversion from pixel to µm, of the centres of all the detected blobs.

The detected coordinates of each fluorescent cells were processed using Python numerical and statistical analysis script, utilising Numpy, Pandas and Scipy libraries. Data points of the blobs were firstly filtered for outliers. We considered blobs that were too big or too small (compared to the median

blob size) to be cells, and blobs that were detected outside of the region covered by the fluorescent cells (i.e. their distance from the centre of mass of the data points was too big or too small compared to the median distance) as the outliers. We used a median-deviation filtering technique to filter the outliers. For a statistical series $s = s_{1,\dots},s_n$, which in this paper would be the series of the blob radii or the series of distances from the centre of mass, the deviation (d_m) from the median value (median(s)), was defined as:

$$d_m(i) = |s_i - \text{median}(s)|$$

The modified z-score was calculated according to:

$$z_{score} = 0.6745 * \frac{d_m}{\text{median}(d_m)}$$

where median(d_m) is the median of absolute deviation. To filter out the outliers, a maximum threshold value of 3.5 was applied as such only points of the series with z-score below 3.5 were retained (Iglewicz et al., 1993).

To determine the spheroid compactness, the distance between nearest neighbour nuclei was calculated from the phalloidin/Hoechst light-sheet images. For each single point representing a Hoechst fluorescent cell nucleus, we computed the nearest neighbour from the remaining data points and recorded the corresponding distance. The resulting series contains the nearest neighbour distances for each cell (with 2 occurrences recorded for each cell, which doesn't affect the actual distribution). The kernel density estimation of this series was then calculated using the gaussian_kde function from the Scipy.stats module. This function relies on a classic probability density functions (PDF) estimation based on the Gaussian kernels of bandwidth $n^{-1/5}$ defined by Scott's law for a 1-dimensional sample of size n.

The PDFs were plotted against the nearest-neighbour distance values to show the distribution of the nearest neighbour distances within each spheroid. The abscissa corresponding to the maximum of the PDF was recorded as a quantitative representation of the spheroid compactness, whereby a lower value represented a more compact spheroid. For both 3D bioprinted and manual spheroid sets, the global distribution functions were calculated as the arithmetic average of the individual spheroid's PDF of the corresponding set. Therefore, we considered all spheroids as statistical entities and give them equal importance in the average. This was in contrast to a statistical analysis of the concatenated dataset of nearest neighbour distances that would skew the results towards the bigger spheroids. We also highlighted the average compactness and its variability in both 3D bioprinted and manual spheroid sets by calculating the average of the individual spheroids PDFs' maxima and their standard deviation.

Locations of the proliferating cells in a spheroid were analysed from the Ki67/Hoechst stained light-sheet images. To compare the repartition of the Ki67 fluorescing cells between the inner region and periphery of the spheroids having variable geometries and dimensions, the data points were first re-centred around their centre of mass and projected to a sphere with a radius of 1 and centred at the origin (0, 0, 0). This was done by firstly subtracting the average (x, y, z) value from the data points. The resulting (x, y, z) coordinates were normalised against their respective maximum absolute value in both positive and negative directions along each axis according to:

$$(\hat{x}_i)_{1\le i\le N} = \left\{ \frac{x_i}{max|x|_{x<0}} if\ x_i < 0 \quad \frac{x_i}{max|x|_{x>0}} if\ x_i > 0 \right\}$$

Where I is the index of each cell centre. The same formula was used for the y and z.

The distribution of the normalised points was then presented by calculating a kernel density estimation of their distance to the origin. The overall distribution for both 3D bioprinted and manual spheroid was plotted as an arithmetic average of each spheroid's PDF within the corresponding 3D bioprinted or manual experimental set. This plot highlighted the repartition of the proliferating cells between inner region and periphery of each type of spheroid and its variability within each experimental set.

To quantify the doxorubicin penetration profile from the CZI microscope image set, comprising a set of bright-field and doxorubicin fluorescent images, we first selected the plane with the highest doxorubicin fluorescence intensity from the z-stack of the doxorubicin channel. Blob detection was then carried out

on the corresponding bright field image to assign an approximated circular geometrical representation of the spheroid and to determine precisely the centre and the radius of the circle. After obtaining the geometrical characteristic of the spheroid slice, the biggest disc around the blob centre was extracted from the fluorescent image and divided into 100 concentric rings on which the average intensity was computed. The corresponding radial profile was then plotted at each time point to show the accumulation of drug inside the spheroid. The highest intensity reached at the final time point was recorded as a reference high value for the test. For each radial profile, we define the drug penetration distance as the distance between the maximum intensity (on the surface of the spheroid) and a minimum threshold defined as a significant fraction of the maximum. We choose 20% of the maximum as minimum threshold to obtain a strong enough intensity to be differentiated from the background. For comparison, penetration distance at each time point was normalised to the final value, and then averaged within both 3D bioprinted and manual spheroid sets. This produced the doxorubicin penetration distance plot.

High-throughput 3D bioprinting of SK-N-BE(2) spheroids for high-throughput screening
SK-N-BE(2) spheroids for high-throughput screening (HTS) was bioprinted using the bespoke 3D bioprinter equipped with the proprietary fly-by printing logic, developed by Inventia Life Science, that enabled printing of twelve wells in a row simultaneously. For HTS of doxorubicin, a full 96-well plate (Cell-Carrier, Perkin Elmer) of SK-N-BE(2) spheroid inside hydrogel matrix were bioprinted according to the method detailed under the 3D bioprinting of cancer spheroids. Bioprinted spheroids were incubated in 10% FCS/DMEM (with Pen-Strep) at 37 °C/5% CO_2 for 3 days before use. After incubation, the plate was imaged using Operetta (2x objective and bright field channel).

High-throughput bioprinting of SK-N-BE(2) spheroids of different sizes
SK-N-BE(2) spheroids for this study were produced according to the bioprinting method described earlier with a slight modification. To generate the small spheroids, 3 droplets (19 nL/droplet) of cell-laden ink were printed, while 7 droplets (19 nL/droplet) of cell-laden ink were bioprinted to generate the large spheroids. The two different spheroid sizes were bioprinted into a 96-well plate (Cell-Carrier, Perkin Elmer), with 48 small spheroids bioprinted in row A-D and 48 large spheroids printed in row E-H. The plate was incubated for 3 days at 37 °C/5% CO_2. After incubation, the plate was imaged using Operetta (2x objective and bright field channel).

High-throughput bioprinting of spheroids in different hydrogel matrix cup sizes
SK-N-BE(2) spheroids for this study were produced according to the bioprinting method described earlier. To vary the hydrogel matrix enclosure size (or cup size) around the spheroid, the bioink microvalve opening time was varied, while keeping other printing parameters constant. The following opening time, 150, 135, 125 and 115 ck were used to generate a cup size around 380 nm, 450 nm, 550 nm and 630 nm, respectively. Five droplets of cell-laden ink (19 nL/droplet) were still printed into each cup. After bioprinting, 200 µL of 10% FCS/DMEM was added into each well and the plate was incubated for 3 days.

HTS of Doxorubicin response of the bioprinted spheroids
Initially, Doxorubicin solutions at 0.125, 0.5, 1, 2, 4, 8 or 32 µM were prepared by mixing doxorubicin (Teva Pharmaceutical) in 10% FCS/DMEM. The solution was prepared fresh prior to each experiment. After incubating the bioprinted spheroids for 3 days, the incubating media was replaced with 200 µL doxorubicin solution. For every doxorubicin concentration, at least 3 wells were prepared. The plate was then incubated for 3 days.

For HTS of doxorubicin, a full 96-well plate of bioprinted spheroids were used to determine the doxorubicin IC_{50}. After 3 days of incubation after bioprinting, the incubating media was replaced with 200 µL doxorubicin in 10% FCS/DMEM at various concentration, in the following arrangement: 0 µM in row A, 0.125 µM in row B, 0.5 µM in row C, 1 µM in row D, 2 µM in row E, 4 µM in row F, 8 µM in row G, 32 µM in row H. The plate was then incubated for 3 days. The effect of doxorubicin was then quantitatively assessed using CellTiter-Glo® endpoint analysis as described earlier. Dose response curve for each experiment was generated in GraphPad Prism software followed by calculation of IC_{50}.

Study of the effect of the hydrogel matrix on SK-N-BE(2) spheroid response to doxorubicin
Bioprinted SK-N-BE(2) spheroids were prepared as described earlier in a 96-well plate (Cell-Carrier, Perkin Elmer). After incubating the plate for 3 days, non-embedded bioprinted SK-N-BE(2) spheroid samples were prepared by recovering the spheroids from the hydrogel matrix by following the method described earlier. The remaining embedded bioprinted spheroids in the well plate were exposed to 200

µL of doxorubicin in 10% FCS/DMEM at various concentration (0, 0.125, 0.5, 1, 2, 4, 8 or 32 µM). In a solid round bottom, white-walled 96-well plate (Costar), 200 µL of doxorubicin in 10% FCS/DMEM at various concentration (0, 0.125, 0.5, 1, 2, 4, 8 or 32 µM) was added. Into each well, one recovered 3D bioprinted spheroid was carefully transferred using a pipette. Both plates were incubated for 3 days at 37 °C/5% CO_2. Quantification was then conducted using CellTiter-Glo® 3D endpoint readout using the method and analysis method as described earlier.

Statistical analysis

Statistical analyses were performed using the GraphPad Prism v6 software (GraphPad Software). Unpaired, two-tailed Student's t-tests were used to determine statistical differences between a control and an experimental group. For comparison of multiple samples, one-way ANOVA with a post hoc Bonferroni test was used. P-values of <0.05 were deemed statistically significant. Results were expressed as means of the number of independent experiments performed (at least 2) ± standard error of mean (SEM).

Prior to conducting strictly standardised mean difference (SSMD) analysis, visual inspection of the HTS data was conducted and outliers were omitted, whereby outliers were described as samples with either no spheroid present or more than one spheroid present. SSMD analysis was conducted according to the method described previously, according to:

$$\mathrm{SSMD} = \frac{\mathrm{mean}(\mathrm{C_{pos}}) + \mathrm{mean}(\mathrm{C_{neg}})}{\sqrt{\mathrm{std}(\mathrm{C_{pos}})^2 + \mathrm{std}(\mathrm{C_{neg}})^2}}$$

where, mean(C_{pos}) and mean(C_{neg}) were the mean of the positive and negative controls respectively and std(C_{pos}) and std(C_{neg}) were the standard deviation of the positive and negative controls respectively. For Exp 1 – 4, SSMD analysis was conducted on a minimum of 10 out of 12 samples (min. n = 10), while 6 out 6 samples (n = 6) were used for Exp 5 – 9.

Supplemental References

Fife, C. M., Sagnella, S. M., Teo, W. S., Po'uha, S. T., Byrne, F. L., Yeap, Y. Y. C., Ng D. C. H., Davis, T. P., McCarroll, J. A., and Kavallaris, M. (2017). Stathmin mediates neuroblastoma metastasis in a tubulin-independent manner via RhoA/ROCK signaling and enhanced transendothelial migration. Oncogene 36, 501-511.

Weiswald, L. B., Guinebretiere, J. M., Richon, S., Bellet, D., Saubamea, B., and Dangles-Marie, V. (2010). In situ protein expression in tumour spheres: development of an immunostaining protocol for confocal microscopy. BMC Cancer 10, 106.

Bradski, G. (2008). Dr. Dobb's Journal of Software ToolsThe OpenCV Library).

Iglewicz, B., and Hoaglin, D. C. (1993). How to Detect and Handle Outliers (ASQC Quality Press).